PAPER • OPEN ACCESS

Experimental study of a high current electromagnetic interference filter for the spacecraft power bus

View the article online for updates and enhancements.

Experimental study of a high current electromagnetic interference filter for the spacecraft power bus

Y S Zhechev, V P Kosteletskii and A M Zabolotsky

Scientific Research Laboratory of Basic Research on Electromagnetic Compatibility, Tomsk State University of Control Systems and Radioelectronics, 40 Lenin Avenue, Tomsk 634050, Russian Federation

E-mail: zhechev75@gmail.com

Abstract. Secondary power supplies, including on-board electronic equipment, extend the range of operating frequencies in order to increase the efficiency of the converters. This leads to the deterioration of electromagnetic environment. We propose a protective device for the spacecraft power bus based on lumped elements, which is characterized by high reliability, radiation resistance, and low mass-dimensional parameters. This device suppresses common and differential conducted interference in high-current power circuits. The results of the circuit simulation and field experiments in the frequency domain are presented. The obtained results are analysed, and the practical recommendations are given regarding the design of noise-suppressing devices based on elements with lumped parameters.

1. Introduction

At present, the importance of providing noise immunity to industrial radio-electronic equipment (REE) including on-board REE of the spacecraft is increasing. The power supply system (PSS) is the main one for any spacecraft, and its electromagnetic compatibility (EMC) should attract great attention because the failure of the electronic system at the power level leads to the failure of the system as a whole [1]. PSS is a set of primary and secondary sources of current or voltage. Advanced satellites are equipped with energy effective and high-efficiency PSS that continuously regulate the power of primary sources [2]. The maximum efficiency is obtained by using non transformer DC voltage converters at high conversion frequencies. However, due to the limited range of regulation, it is difficult to match the voltage levels of the power supplies used [3]. Inverter and transformer circuits are used to implement the maximum performance mode during the whole life cycle of the satellite [4]. In this case, power supply voltage levels are arbitrarily matched to the load. The use of inverter-transformer converters based on a current inverter in the spacecraft PSS makes it possible to regulate the output voltage of primary power supplies in a wide range, thus realizing extreme power control [5]. However, the increase in conversion efficiency negatively affects electromagnetic environment. Transient processes formed during the operation of voltage converters, switching, and transmitting equipment generate broadband radiated and conducted interference [6, 7]. They are able to penetrate deep into the radio-electronic equipment and disable it through the output bus unit that serves to distribute electricity between on-board equipment in the PSS of the spacecraft. Previous works have presented the spacecraft power bus that provides power supply to different units of the vehicle with a total power of 20 kW (Figure 1).

Figure 1. Spacecraft power bus.

In [8], the influence of the power bus cross-section on its characteristics has been investigated. The optimal geometrical parameters with minimum parasitic inductance have been determined. The paper [9] presents the results of the quasi-static simulation of the power bus and the side conductors connected to it. Since the power bus under consideration is one of the main elements of the spacecraft PSS, its crosstalk immunity and reliability is important [10]. For example, to protect the bus against electrostatic discharge, conductive tapes made of aramid threads with a copper silvered wire winding are used. Shielding is used to limit the levels of radiated electromagnetic noise. To protect against conducted electromagnetic noise, interference suppression filters are used. To provide EMC of onboard REE, it is advisable to use passive filters with high reliability, radiation resistance and low weight characteristics.

2. Problem statement
To limit the levels of common mode (CM) and differential mode (DM) conducted noise for the power bus, in [11] we have proposed a noise suppression low-pass filter with the third order Butterworth characteristic. This class of filtering devices has the flattest possible amplitude-frequency response in the bandwidth. This device includes passive RLC-components of surface mounting. As opposed to active noise protection devices, there are no active or semiconductor components in this filter. Therefore, our device has the required reliability. However, the low current-carrying capability does not allow this noise suppression filter to be used in the power bus. In [12], we have proposed a new high-current filter that meets the requirements for current throughput. As the results of simulation and experimental study of this device have not been presented before, the purpose of this work is to fill this gap. For this, it is necessary to construct a mathematical model of the developed EMI-filter, to carry out experimental study, to compare the obtained CM and DM frequency characteristics, and to analyse the obtained results.

3. Approaches, methods and design
Figure 2 shows an equivalent circuit diagram of the EMI-filter (ports 1 and 3 are input, ports 2 and 4 are output). It is designed to limit the level of conducted emissions from secondary power supplies. Capacitors C_{DM1} and C_{DM2} are designed to attenuate DM interference. To limit the reactive power consumed from the power supply at the design stage, we chose a small value of C_{DM2} capacitor. Chokes L_{DM1} and L_{DM2} are two uncoupled coils on ring ferrite cores. They are designed to suppress CM and DM interferences. Capacitors C_{CM1} and C_{CM2} are designed to suppress both CM and DM interferences. When selecting their values, it is important to pay attention to the allowable reactive leakage currents. CM choke L_{CM1} represents two coils wound in one direction on a common core. We used ring ferrite as a core. When DM currents flow through the coils, the magnetic fields induced by these currents are directed oppositely to each other and the total magnetic flux is zero. If the resistance of the coils is not taken into account, then, with absolute symmetry of the coils, the input impedance of such systems is zero. The inductor has no effect on the flow of DM currents. In the case of CM currents, the magnetic fluxes of the coils are co-directional. Thus, they are added up and the input impedance of such system increases. This leads to the suppression of currents caused by CM interference and a significant reduction in the amplitude of the interference signal.
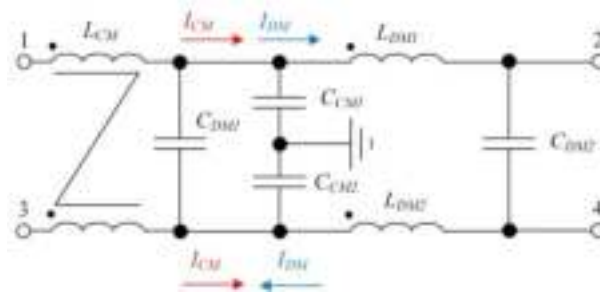
Figure 2. Equivalent circuit diagram of the EMI-filter.

In this paper, the authors used circuit simulation implemented in the computer program LTspice, which uses an algorithm for simulating the processes occurring in electronic circuits. It is based on a modified nodal potential method. This approach allows one to refine and optimize the results of preliminary calculations, and empirically select component parameters and different circuit operation modes. At frequencies above 10 MHz, parasitic parameters of circuit elements and wiring begin to significantly influence the frequency characteristics. Therefore, above 10 MHz, the error of the obtained circuit simulation results increases. Figure 3 shows a prototype EMI-filter for the experimental study. It has the following weight and size characteristics: the length is 70 mm, the width is 40 mm, the height is 12 mm, and the weight is 31 g. The filter is a symmetrical device relative to the lengthwise axis. In addition to the optimal layout of the filter elements, it improves CM interference suppression by the conductor topology. The EMI-filter must provide a current of 10 A. Thus, the required cross-section of the conductor should be at least 1.1 mm^2.
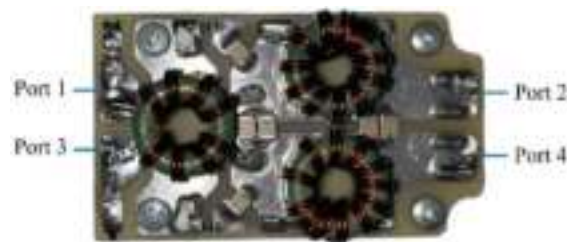
Figure 3. Prototype of EMI-filter for the spacecraft power bus.

Figure 4 presents double layer printed circuit board layers of the EMI-filter in which the topology of its conductors is clearly visible. The conductors of the EMI-filter are implemented in polygons of a complex shape, which allows increasing the margin for the current load, mechanical strength, and provides additional heat dissipation.

Figure 5 shows a block diagram of a measurement setup used for measuring frequency characteristics. The unit consists of a scalar circuit analyser with the VSWR sensor and the detector head connected to its measuring inputs. The EMI-filter is installed between them as a device under test.

a   b
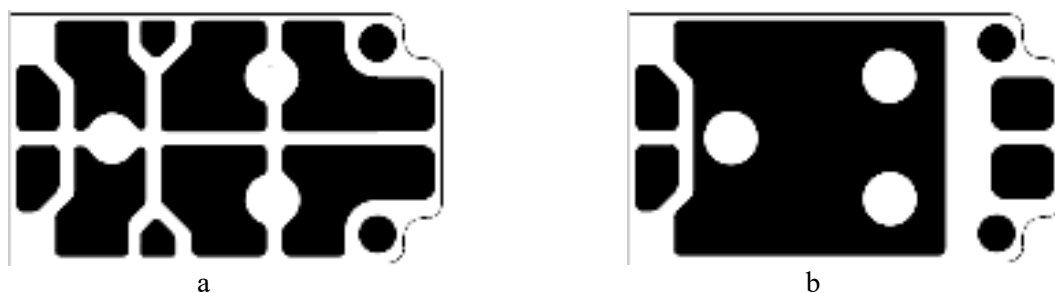
Figure 4. Top (a) and bottom (b) layers of the EMI-filter prototype.
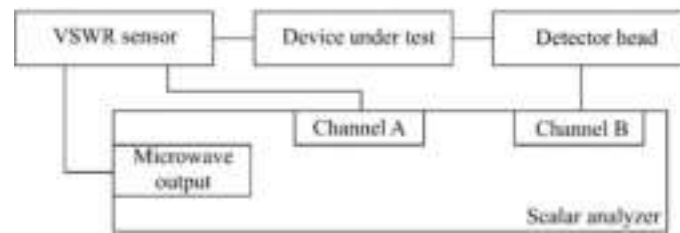
Figure 5. Block diagram of the measurement setup.

The developed EMI-filter is a four-port device; therefore, to correctly extract its amplitude-frequency characteristics, the technique of balanced measurements from [13] was applied. The authors used unbalanced frequency response to calculate the balance characteristics of the device under study. The expressions for calculating the balance characteristics (transmission coefficients) for the CM and DM are presented as

$$S_{cc21} = \frac{S_{21} + S_{41} + S_{23} + S_{43}}{2},$$ (1)

$$S_{dd21} = \frac{S_{21} - S_{41} - S_{23} + S_{43}}{2}.$$ (2)

4. Results

Figures 6 and 7 show simulation and experimental results for the frequency range from 0 to 10 MHz in the CM and DM, respectively. The results show the frequency dependence of the attention ratio $|S_{21}|$ for both modes. The calculated and measured cut frequencies for both modes are shown in Table 1. From the graphs we can see that the forms of the curves obtained agree well. For example, the absolute deviation of the cut frequency for the common mode was 0.4 kHz. In the frequency range from 0.5 to 10 MHz the attenuation was at least 60 dB for experimental data and simulation.

In the case of the DM, we can also see that the curves are similar in nature. However, in the frequency range from 0.01 to 0.09 MHz in the experiment, there is a drop due to resonances of the test object. In the frequency range from 0.5 to 10 MHz, the attenuation was at least 80 dB for experimental data and simulation.
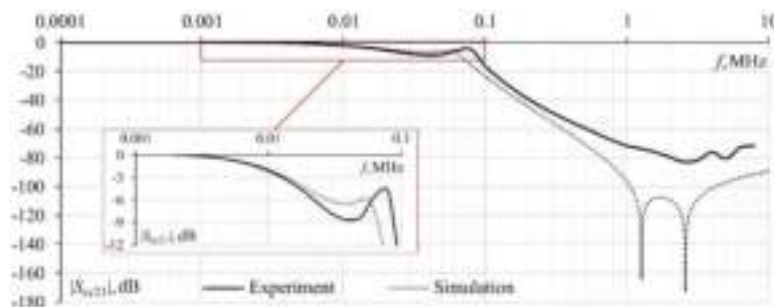
Figure 6. Frequency dependence of $|S_{21}|$ of the EMI-filter in the CM up to 10 MHz.
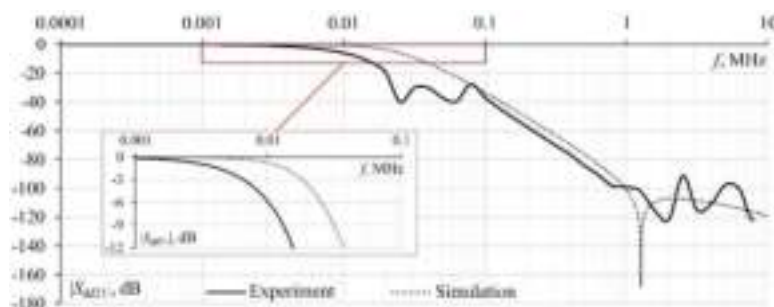
Figure 7. Frequency dependence of $|S_{21}|$ of the EMI-filter in the DM up to 10 MHz.

Table 1. Comparison of calculated and measured cut frequencies for CM and DM.

Parameters	Simulation, kHz	Experiment, kHz	Absolute deviation, kHz
Cut frequency in CM	13.6	14.0	0.4
Cut frequency in DM	18.0	6.8	11.2

Figures 8 and 9 show the results of simulation and experimental study in the frequency range from 10 to 1000 MHz in the CM and DM, respectively. One can see from both graphs that parasitic parameters of mounting and components have a considerable influence on the frequency response. The largest deviation between the results of the experimental study and the simulation was due to unaccounted parasitic parameters of the components of the EMI-filter PCB and its connectors. In the frequency range from 10 to 1000 MHz the attenuation for the CM was at least 15 dB and for the DM – 22 dB.

From the presented graphs, we can see that the investigated device is a low-pass filter for CM and DM. The device has a wide suppression band for both modes. The minimum attenuation is 15 and 22 dB for CM and DM, respectively. The following parameters should be taken into account when designing noise suppressors for the spacecraft power bus: current-carrying capacity, cut-off frequencies in CM and DM, leakage currents and mass-dimensional characteristics. To carry out preliminary calculations of such devices, it is recommended to use a schematic approach. However, to analyse them at frequencies above 10 MHz, it is necessary to use multi-resonance models of the EMI-filter components.
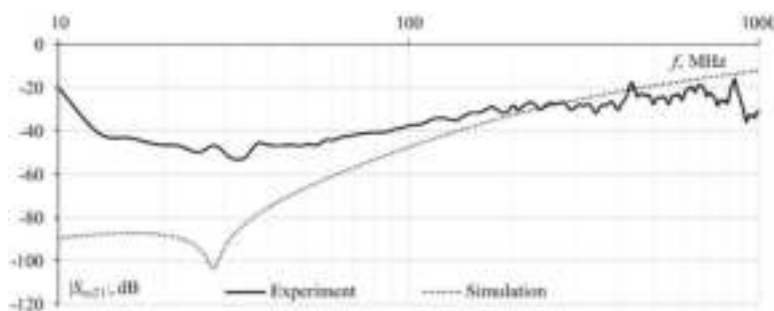
Figure 8. Frequency dependence of $|S_{21}|$ of the EMI-filter in the CM from 10 to 1000 MHz.
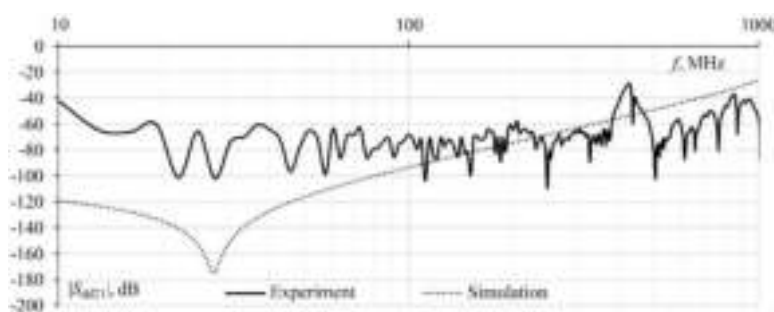
Figure 9. Frequency dependence of $|S_{21}|$ of the EMI-filter in the DM from 10 to 1000 MHz.

5. Conclusion
To increase the efficiency of converters, secondary power sources, including on-board electronic equipment, we extend the range of operating frequencies. This leads to the deterioration of electromagnetic environment. The work presents a protective device for the spacecraft power bus based on the elements with lumped parameters, which is characterized by increased reliability, radiation immunity and low mass-dimensional parameters. The designed prototype of the EMI-filter is able to suppress CM and DM conductive electromagnetic interferences. The work included circuit simulation in frequency ranges from 0 to 10 MHz and from 10 to 1000 MHz. Experimental study and comparative

analysis of $|S_{21}|$ frequency dependence for CM and DM were carried out. The simulation and experimental results show that the EMI-filter successfully performs its job. In addition, this device has small mass-dimensional characteristics, which is relevant for the spacecraft power bus. It should be noted that the EMI-filter is implemented without using active components, which allows prolonging its lifetime and significantly reducing the probability of failure caused by the radiation background of space. As a final result, the developed EMI-filter is integrated into the prototype spacecraft power bus and has passed full-scale tests.

References
[1] Zhadnov V and Artyukhova M 2015 *Dependability* 13–24
[2] Shinyakov Y 2006 *Bulleten of the Tomsk Polytechnic University. Geo Assets Engineering* **309**
[3] Osipov A, Shurygin Y, Shinyakov Y, Otto A and Chernaya M 2013 *Proceedings of Tomsk State University of Control Systems and Radioelectronics*
[4] Osipov A, Shinyakov Y, Otto A and Chernaya M 2013 *Bulleten of the Tomsk Polytechnic University. Geo Assets Engineering* **323**
[5] Osipov A, Shinyakov Y, Otto A, Chernaya M and Tkachenko A 2014 *Bulleten of the Tomsk Polytechnic University. Geo Assets Engineering* **324**
[6] Luo F L and Ye H 2018 *Power electronics: advanced conversion technologies* (CRC press)
[7] Lehr J and Ron P 2017 *Foundations of pulsed power technology* (John Wiley & Sons)
[8] Ternov S, Demakov A and Komnatnov M 2018 *2018 Moscow Workshop on Electronic and Networking Technologies (MWENT)* (IEEE) pp 1–4
[9] Kuksenko S 2019 *Trudy MAI* 21–21
[10] Erickson R W and Maksimovic D 2007 *Fundamentals of power electronics* (Springer Science & Business Media)
[11] Zhechev Y, Kosteletskii V, Zabolotsky A and Gazizov T 2019 *IOP Conference Series: Materials Science and Engineering* vol 560 (IOP Publishing) p 012133
[12] Zhechev Y and Kosteletskii V 2019 *18th International Conference "Aviation and Cosmonautics – 2019"* pp 121–122
[13] Dunsmore J P 2020 *Handbook of microwave component measurements: with advanced VNA techniques* (John Wiley & Sons)